Journal of Engineering and Applied Sciences 5 (1): 19-29, 2010
ISSN: 1816-949X

General Newtonian Flow Due to the Longitudinal and Torsional Oscillation of a Rod

[1]Amanda Rambaran and [2]Karim Rahaman
[1]School for Studies in Learning, Cognition and Education,
The University of Trinidad and Tobago, Corinth Campus, Corinth Road,
San Fernando, Trinidad, Republic of Trinidad and Tobago
[2]Department of Mathematics and Computer Science,
Faculty of Science and Agriculture, The University of the West Indies,
St. Augustine, Trinidad, Republic of Trinidad and Tobago

Abstract: The unsteady flow of an incompressible viscous fluid, characterized by the motion of a long, circular, cylindrical rod, oscillating both longitudinally and torsionally at different frequencies and amplitudes isexamined, with slip occurring at the surface of the cylindrical rod. Analytical expressions for the velocity field, the tangential drag and the work done by the drag force have been obtained and are displayed graphically using particular values of the flow parameters. These are plotted for different values of slip from perfect slip to no-slip, so as to get some insight into the effects of slip.

Key words: Oscillation, viscous, longitudinal, torsional, different frequencies, different amplitudes, slip

INTRODUCTION

Casarella and Laura (1969) investigated the motion of a viscous fluid due to the longitudinal and torsional oscillation of an infinite circular cylindrical rod immersed in a fluid. They were primarily interested in the drag force acting on the rod as this is of practical significance in many ocean engineering problems. They obtained exact solutions for the velocity field, stresses and drag on the rod. Rajagopal (1983) examined a similar problem for a non-Newtonian fluid in particular a fluid of second grade and like Casarella and Laura, obtained an exact solution to the field equation. Ramkissoon and Majumdar (1990) examined the corresponding internal flow problem for viscous fluids. They obtained an exact solution for the flow field and explicit expressions were given for the shear stresses, the drag experienced by the cylinder and the drag coefficient. Ramkissoon *et al.* (1991) examined the same problem as Casarella and Laura (1969) but for a Polar fluid. Here, an exact solution was obtained for the velocity field. Rahaman (2004, 2005) examined the same problem as Ramkissoon and Majumdar (1990) and Casarella and Laura (1969) but for an upper-convected Maxwell fluid, explicit expressions were obtained for the velocity field, shear stresses and drag in each case. In all of these problems, the frequencies of oscillations in the longitudinal and torsional directions were the same. Furthermore, the magnitude of the oscillations contained a common parameter, implying dependency for these orthogonal motions.

Owen and Rahaman (2006) appear to be the first to relax the common oscillatory frequencies for the two directions of motion in their internal flow problem examined and thus took different frequencies for these oscillations.

The main objective of this research is to investigate a similar problem to that of Casarella and Laura (1969) for a viscous fluid but a more general case. In particular, the motion of a viscous fluid due to the longitudinal and torsional oscillation of an infinite, circular cylindrical rod immersed in the fluid is examined but the two different oscillations of the rod are moving with different frequencies, like that done by Owen and Rahaman (2006). Further, the amplitude dependency of the oscillatory motions, due to the presence of a common factor is removed. Finally, slip at the surface of the cylindrical rod is taken into consideration, as it has long been established that the conventional no-slip boundary condition begins to break down even before the linear stress-strain relationship becomes invalid (Gad-el-Hak, 1999).

Schaaf and Chambre (1961) have shown that the slip parameter, β, otherwise known as the Coefficient of Sliding Friction is given by Eq. 1:

Corresponding Author: Amanda Rambaran, School for Studies in Learning, Cognition and Education, The University of Trinidad and Tobago, Corinth Campus, Corinth Road, San Fernando, Trinidad, Republic of Trinidad and Tobago

$$\beta = \frac{\mu}{\left(\frac{2-\sigma}{\sigma}\right)LKn} \quad (1)$$

Where:

μ = The viscosity coefficient
σ = The Tangential Momentum Accommodation Coefficient (TMAC)
L = The characteristic length of the flow geometry
Kn = The Knudsen number, which determines the degree of rarefaction effects and the validity of the continuum hypothesis

It can be shown that $Kn \geq 0$ and when $Kn \geq 0.1$, the continuum model and therefore the Navier-Stokes equations become invalid in which case, the Boltzman equation has then to be applied to describe the molecular motion properly. When $Kn \geq 0.01$, the Navier-Stokes equation is a good approximation. However, when $0.01 \leq Kn \geq 0.1$ (commonly referred to as the slip-flow regime), the Navier-Stokes equations can still be used, provided tangential slip-velocity boundary conditions are implemented along the solid walls of the flow domain (Schaaf and Chambre, 1961; Aleksandrov *et al*., 1988; Morinishi, 2006). It is the latter situation, i.e., a continuum flow field with slip boundary conditions that is to be investigated in this study.

MATERIALS AND METHODS

A long, straight, solid, circular cylindrical rod with uniform cross-section, of radius a, undergoing oscillations both longitudinally and torsionally with different frequencies and amplitudes and fully immersed in an incompressible viscous fluid is considered. It will be assumed that the rod is infinite in length, so that rod end effects are neglected, no external forces are acting and the flow is fully established, which is at rest at infinity.

The equation of motion for a viscous fluid (Ramkissoon and Majumdar, 1990) is given by the Navier-Stokes equation:

$$\underline{F} - \frac{1}{\rho}\nabla p + \nu\nabla^2\underline{q} = \frac{d\underline{q}}{dt} = \frac{\partial \underline{q}}{\partial t} + (\underline{q}\cdot\nabla)\underline{q} \quad (2)$$

Where:

F = The external force per unit mass
p = The pressure field
ρ = The density of the fluid
$\nu = \mu/\rho$ = The kinematic viscosity in which μ is the viscosity coefficient and q is the velocity field

Working in cylindrical polar co-ordinates (R, θ, z) with the z-axis coinciding with the axis of the cylinder, assuming symmetry, then it is fair to assume that the velocity field of the induced flow is of the form

$$\underline{q} = v(R,t)\hat{\theta} + w(R,t)\hat{z} \quad (3)$$

It is also assumed that the pressure field is independent of the $\hat{\theta}$ and $\hat{z}$ co-ordinates and is of the form:

$$p = p(R,t) \quad (4)$$

The continuity equation for an incompressible fluid is (Ramkissoon and Majumdar, 1990):

$$\nabla\cdot\underline{q} = 0 \quad (5)$$

Substituting Eq. 3 into 2, gives for each component:

$$\hat{R}: -\frac{1}{\rho}\frac{\partial p}{\partial R} = -\frac{v^2}{R} \Rightarrow \frac{\partial p}{\partial R} = \rho\frac{v^2}{R} \quad (6)$$

$$\hat{\theta}: \nu\left(\nabla^2 v - \frac{v}{R^2}\right) = \frac{\partial v}{\partial t} \Rightarrow \frac{\partial v}{\partial t} = \nu\left(\frac{\partial^2 v}{\partial R^2} + \frac{1}{R}\frac{\partial v}{\partial R} - \frac{v}{R^2}\right) \quad (7)$$

$$\hat{z}: \nu\nabla^2 w = \frac{\partial w}{\partial t} \Rightarrow \frac{\partial w}{\partial t} = \nu\left(\frac{\partial^2 w}{\partial R^2} + \frac{1}{R}\frac{\partial w}{\partial R}\right) \quad (8)$$

The components of stress are given by Batchelor (1967):

$$S_{ii} = -p + 2\mu e_{ii} \qquad (i = R,\theta,z) \quad (9)$$

$$S_{ij} = 2\mu e_{ij} \qquad (i \neq j) \quad (10)$$

where, e_{ij} are the components of the rate of deformation tensor, which in this case are given by Batchelor (1967):

$$e_{RR} = 0 \quad (11)$$

$$e_{\theta\theta} = \frac{1}{R}\left(\frac{\partial v}{\partial \theta}\right) = 0 \quad (12)$$

$$e_{zz} = \frac{\partial w}{\partial z} = 0 \quad (13)$$

$$2e_{\theta z} = 2e_{z\theta} = \frac{1}{R}\frac{\partial w}{\partial \theta} + \frac{\partial v}{\partial z} = 0 \quad (14)$$

$$2e_{zR} = 2e_{Rz} = \frac{\partial w}{\partial R} \tag{15}$$

$$2e_{R\theta} = 2e_{\theta R} = \frac{\partial v}{\partial R} - \frac{v}{R} \tag{16}$$

Utilizing Eq. 11-16 in Eq. 9 and 10 gives the components of stress as:

$$S_{RR} = S_{\theta\theta} = S_{zz} = -p \tag{17}$$

$$S_{\theta z} = S_{z\theta} = 0 \tag{18}$$

$$S_{zR} = S_{Rz} = \mu\left(\frac{\partial w}{\partial R}\right) \tag{19}$$

$$S_{R\theta} = S_{\theta R} = \mu\left(\frac{\partial v}{\partial R} - \frac{v}{R}\right) \tag{20}$$

By solving Eq. 7 and 8, subject to certain conditions, the velocity field can be completely determined. Note that when the velocity field has been determined, the pressure field and the components of stress can also be determined from Eq. 4, 6, 19 and 20.

The velocity of the rod at its surface is taken to be:

$$\underline{u} = \alpha_1\cos(\Omega_1 t)\hat{\theta} + \alpha_2\cos(\Omega_2 t)\hat{z} \tag{21}$$

where, Ω_1, Ω_2 represent the different frequencies in the torsional and longitudinal directions respectively. α_1, α_2 are the different amplitudes of the oscillations in the torsional and longitudinal directions respectively.

For the slip condition at the surface of the rod, the well known condition proposed by Basset (1961) is used that is the tangential velocity of a fluid relative to the solid at a point on its surface is proportional to the tangential stress prevailing at that point. For this it will be assumed that the material making up the surface of the rod is uniform, so that the mean degree of roughness per unit area is the same. This implies that there will be equal amounts of slip in any direction and in particular, the longitudinal and torsional directions.

Using this last assumption, 3, 21 and Basset's slip condition gives:

$$ß\left[v - \alpha_1\cos(\Omega_1 t)\right]_{R=a} = S_{R\theta}\big|_{R=a} \tag{22}$$

and

$$ß\left[w - \alpha_2\cos(\Omega_2 t)\right]_{R=a} = S_{Rz}\big|_{R=a} \tag{23}$$

where, $ß$ is the slip parameter which is assumed to depend only on the nature of the fluid and the solid surface.

Furthermore, $ß \geq 0$ and in particular, $ß = 0$ represents perfect slip, whereas $ß \to \infty$ represents no slip. Using Eq. 19 and 20 in 22 and 23, respectively gives:

$$ß\left[v - \alpha_1\cos(\Omega_1 t)\right]_{R=a} = \mu\left[\frac{\partial v}{\partial R} - \frac{v}{R}\right]_{R=a} \tag{24}$$

and

$$ß\left[w - \alpha_2\cos(\Omega_2 t)\right]_{R=a} = \mu\left[\frac{\partial w}{\partial R}\right]_{R=a} \tag{25}$$

Since the flow is at rest at infinity then:

$$v(R,t) \to 0 \text{ as } R \to \infty \tag{26}$$

and

$$w(R,t) \to 0 \text{ as } R \to \infty \tag{27}$$

To determine the velocity field, q, given by (3), Eq. 7 and 8 need to be solved subject to the conditions given by Eq. 24-27. It is noted that Eq. 3 satisfies the continuity Eq. 5, automatically.

Assume that v(R, t) and w(R, t) are of the form:

$$v(R,t) = \Re[f(R)e^{i\Omega_1 t}] \tag{28}$$

and

$$w(R,t) = \Re[g(R)e^{i\Omega_2 t}] \tag{29}$$

where '$\Re$' represents the real part of the expression.

On substituting these into Eq. 7 and 8 and solving subject to the stated conditions gives:

$$v(R,t) = \Re\left[\frac{\alpha_1 ß K_1(\gamma_1 R)}{\mu\gamma_1 K_0(\gamma_1 a) + \left(ß + \frac{2\mu}{a}\right)K_1(\gamma_1 a)}e^{i\Omega_1 t}\right] \tag{30}$$

and

$$w(R,t) = \Re\left[\frac{\alpha_2 ß K_0(\gamma_2 R)}{ß K_0(\gamma_2 a) + \mu\gamma_2 K_1(\gamma_2 a)}e^{i\Omega_2 t}\right] \tag{31}$$

where:

$$\gamma_j = \sqrt{\frac{i\Omega_j}{\nu}},\ (j = 1,2) \text{ and } K_n(x)$$

is the Modified Bessel Function of the second kind of order n. The fluid's velocity field has now been completely determined.

Utilizing Eq. 30 and 31 in Eq. 20 and 19, respectively, the shear stresses on the rod are found to be:

$$S_{R\theta} = \Re\left[\frac{-\mu\gamma_1\alpha_1\beta\left(K_0(\gamma_1 a)+\frac{2K_1(\gamma_1 a)}{\gamma_1 a}\right)}{\mu\gamma_1 K_0(\gamma_1 a)+\left(\beta+\frac{2\mu}{a}\right)K_1(\gamma_1 a)}e^{i\Omega_1 t}\right] \quad (32)$$

and

$$S_{Rz} = \Re\left[\frac{-\mu\gamma_2\alpha_2\beta K_1(\gamma_2 a)}{\beta K_0(\gamma_2 a)+\mu\gamma_2 K_1(\gamma_2 a)}e^{i\Omega_2 t}\right] \quad (33)$$

The tangential drag force, $\underline{D}$, acting on the rod per unit length is (Casarella and Laura, 1969):

$$\underline{D} = -2\pi a[S_{R\theta}\hat{\theta} + S_{Rz}\hat{z}]_{R=a} \quad (34)$$

Substituting Eq. 32 and 33 into 34 gives:

$$\underline{D} = 2\pi a\mu\beta\Re\left[\begin{array}{c}\frac{\gamma_1\alpha_1\left(K_0(\gamma_1 a)+\frac{2K_1(\gamma_1 a)}{\gamma_1 a}\right)}{\mu\gamma_1 K_0(\gamma_1 a)+\left(\beta+\frac{2\mu}{a}\right)K_1(\gamma_1 a)}e^{i\Omega_1 t}\hat{\theta}+\\ \frac{\gamma_2\alpha_2 K_1(\gamma_2 a)}{\beta K_0(\gamma_2 a)+\mu\gamma_2 K_1(\gamma_2 a)}e^{i\Omega_2 t}\hat{z}\end{array}\right] \quad (35)$$

The work done W_j by the drag force $\underline{D}$ on the fluid per half-cycle of torsional and longitudinal motion is given by Casarella and Laura (1969):

$$W_j = -\int_0^{\frac{\pi}{\Omega_j}} \underline{D}\cdot\underline{u}\,dt \quad (36)$$

where, j = 1, 2 refer to the torsional and longitudinal motions respectively.

Substituting Eq. 21 and 35 into 36 gives:

$$W_j = -\pi a\mu\beta\Re\left[\begin{array}{c}\frac{\gamma_1\alpha_1^2\left(K_0(\gamma_1 a)+\frac{2K_1(\gamma_1 a)}{\gamma_1 a}\right)}{\mu\gamma_1 K_0(\gamma_1 a)+\left(\beta+\frac{2\mu}{a}\right)K_1(\gamma_1 a)}\hat{I}(\Omega_j,\Omega_1)+\\ \frac{\gamma_2\alpha_2^2 K_1(\gamma_2 a)}{\beta K_0(\gamma_2 a)+\mu\gamma_2 K_1(\gamma_2 a)}\hat{I}(\Omega_j,\Omega_2)\end{array}\right] \quad (37)$$

where:

$$\hat{I}(\Omega_j,\Omega) = 2\int_0^{\frac{\pi}{\Omega_j}} e^{i\Omega t}\cos(\Omega t)dt = \frac{\Omega_j\cos\left(\frac{\pi\Omega}{\Omega_j}\right)\sin\left(\frac{\pi\Omega}{\Omega_j}\right)+\pi\Omega-i\Omega_j\cos^2\left(\frac{\pi\Omega}{\Omega_j}\right)+i\Omega_j}{\Omega\Omega_j} \quad (38)$$

RESULTS AND DISCUSSION

In order to get some insight on the effects of slip, various graphs involving the components of velocity, drag force and work done are displayed for different values of the slip parameter β, ranging from β = 0 (perfect slip) to β→∞ (no-slip). For some practical oceanographic problems, the parameters ν and Ω_j are bounded by Casarella and Laura (1969):

$$9.30\times10^{-7} \le \nu \le 1.86\times10^{-6}\ \text{m}^2\ \text{sec}^{-1} \quad (39)$$

$$1 \le \frac{\Omega_j}{2\pi} \le 10\ \text{Hz} \quad (40)$$

Following Casarella and Laura by taking:

$$\sqrt{\frac{\Omega_j}{\nu}}\,a = 112 \quad (41)$$

gives on substituting into Eq. 40:

$$\frac{3136\nu}{5\pi} \le a^2 \le \frac{6272\nu}{\pi}\ \text{m}^2 \quad (42)$$

For seawater, $\nu = 1.17\times10^{-6}\ \text{m}^2\ \text{sec}^{-1}$ and $\mu = 0.00121$ pas (LMNO Engineering, Research and Software, Ltd., 1999), substituting this value of ν into Eq. 42 gives approximately:

$$0.0153 \le a \le 0.0483\ \text{m} \quad (43)$$

Using Eq. 43, the value of a is taken to be:

$$a = 0.03\ \text{m} \quad (44)$$

Using Eq. 41 with j = 1, Eq. 44 and ν for seawater, gives approximately:

$$\Omega_1 = 16.3 \quad (45)$$

Taking into consideration the minimum value of:

$$\sqrt{\frac{\Omega_1}{\nu}}a \approx 5.05$$

for a 0.00635 m diameter rod, as stated by Casarella and Laura, then selecting:

$$\sqrt{\frac{\Omega_2}{\nu}}a = 75 \quad (46)$$

along with Eq. 44 and ν for seawater, gives approximately:

$$\Omega_2 = 7.31 \quad (47)$$

The behaviour of the velocity profiles of the $\hat{\theta}$-component are displayed in Fig. 1-4 for four different values of the slip parameter β. As observed, the magnitude of the velocity decreases as one moves away from the cylindrical rod, however, the larger the value of β then the greater the magnitude of ν (R, t)/α_1. The same is observed in Fig. 5-8 for w (R, t)/α_2 from the $\hat{z}$-component.

Figure 9-12 show the behaviour of the velocity profiles of the $\hat{\theta}$-component at four different times. As observed, the magnitude of the velocity decreases as one

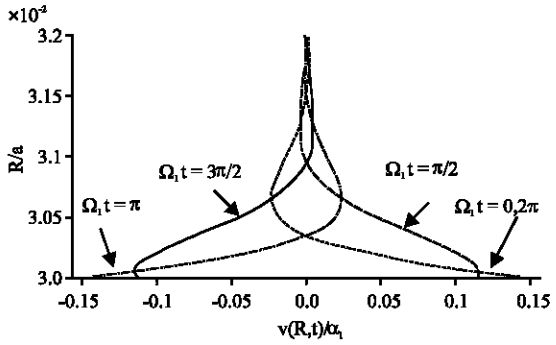

Fig. 1: v(R, t)/α_1 for β = 1

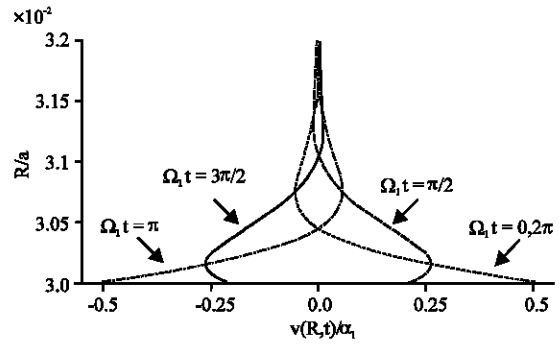

Fig. 2: v(R, t)/α_1 for β = 5

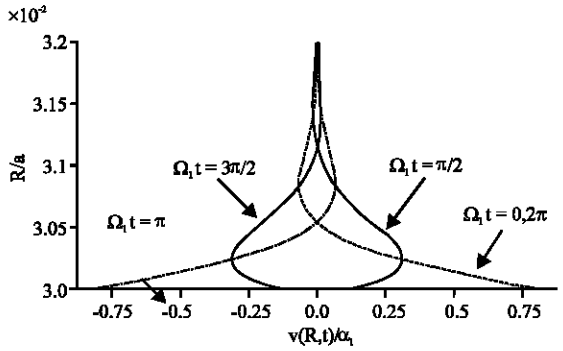

Fig. 3: v(R, t)/α_1 for β = 20

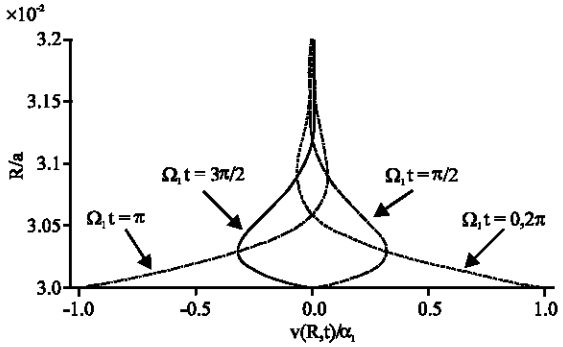

Fig. 4: v(R, t)/α_1 for β →∞

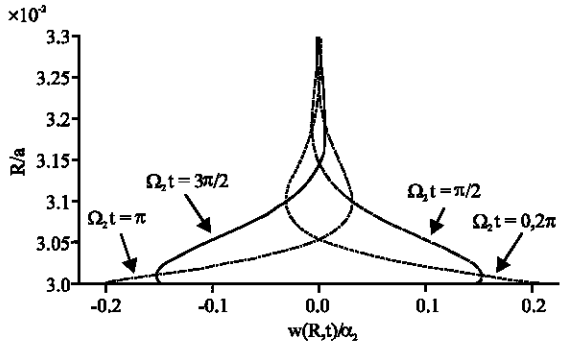

Fig. 5: w(R, t)/α_2 for β = 1

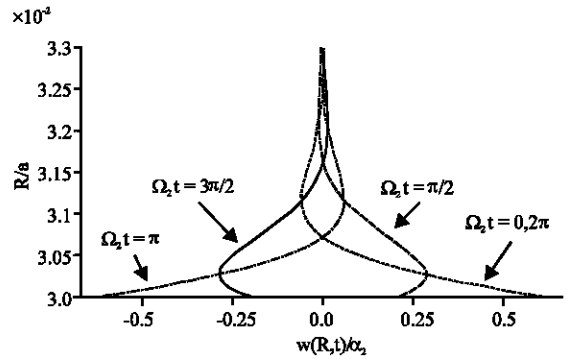

Fig. 6: w(R, t)/α_2 for β = 5

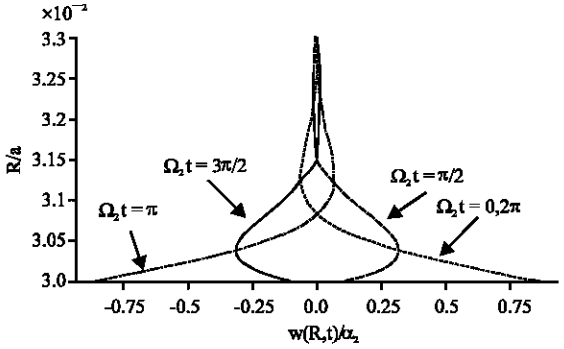

Fig. 7: $w(R, t)/\alpha_2$ for $\beta = 20$

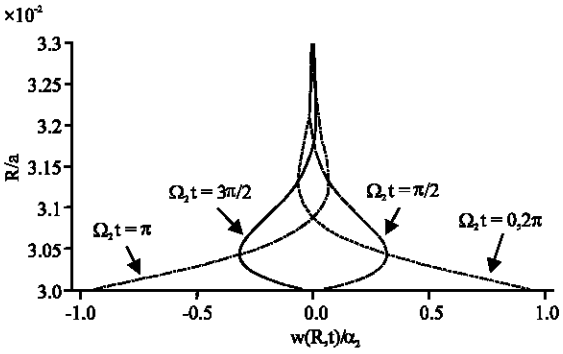

Fig. 8: $v(R, t)/\alpha_2$ for $\beta \to \infty$

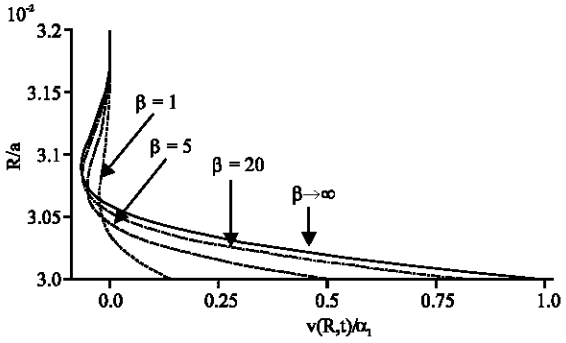

Fig. 9: $v(R, t)/\alpha_1$ for $t = 0$

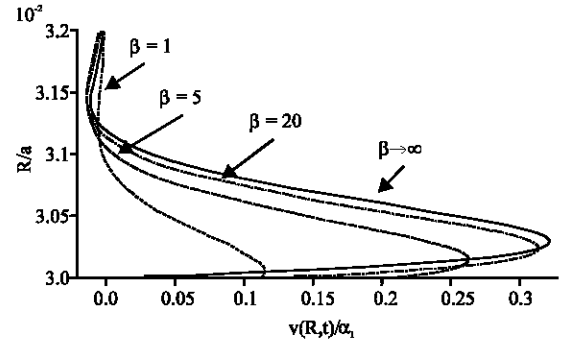

Fig. 10: $v(R, t)/\alpha_1$ for $t = \pi/2\Omega_1$

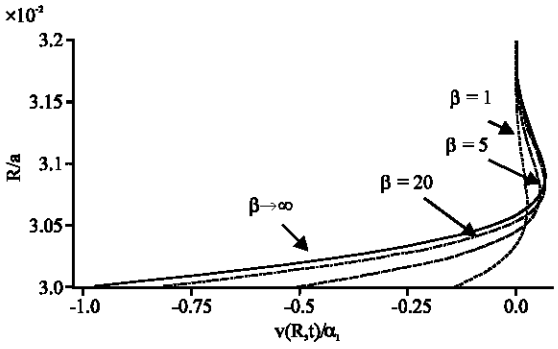

Fig. 11: $v(R, t)/\alpha_1$ for $t = \pi/\Omega_1$

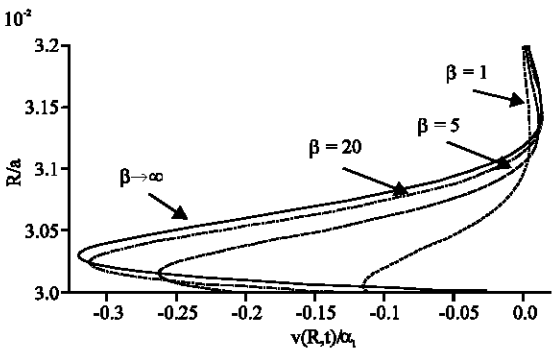

Fig. 12: $v(R, t)/\alpha_1$ for $t = 3\pi/2\Omega_1$

moves away from the cylindrical rod. Also, the larger the value of β then the greater the magnitude of $v(R, t)/\alpha_1$ this is consistent with that observed in Fig. 1-4. The same is observed in Fig. 13-16 for $w(R, t)/\alpha_2$ from the $\hat{z}$-component.

Figure 17 shows the behaviour of the $\hat{\theta}$-component of the velocity field against β for four different values of t on the surface of the cylindrical rod. It can be observed that as β increases, $v(R, t)/\alpha_1$ tends to the no-slip case. In Fig. 18 a similar observation can be made for the behaviour of the $\hat{z}$-component.

With respect to the drag, Fig. 19 shows the behaviour of the $\hat{\theta}$-component against β at four different times. It is observed that as the value of β increases, the magnitude of $\hat{\theta}$-component/α_1 also increases. In Fig. 20, a similar observation is made for the $\hat{z}$-component/α_2. Figure 21 shows the behaviour of the $\hat{\theta}$-component of the drag against t for four different values of the slip parameter β. For each value of β, it can be observed that the graph appears to be periodic and as β increases, the magnitude of the $\hat{\theta}$-component/α_1 also increases, which is consistent with the observations from Fig. 19. Corresponding to Fig. 21, the same observation can be made for the $\hat{z}$-component/α_2 from Fig. 22. This is also consistent with observations from Fig. 20.

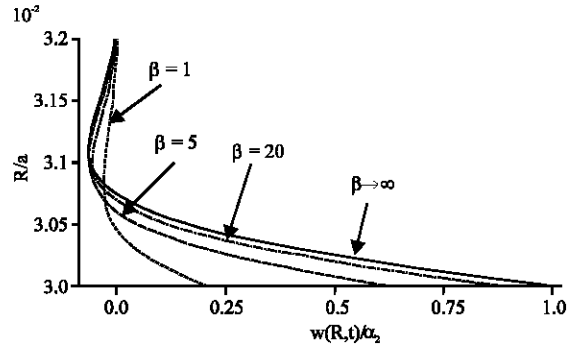

Fig. 13: w (R, t)/α_2 for t = 0

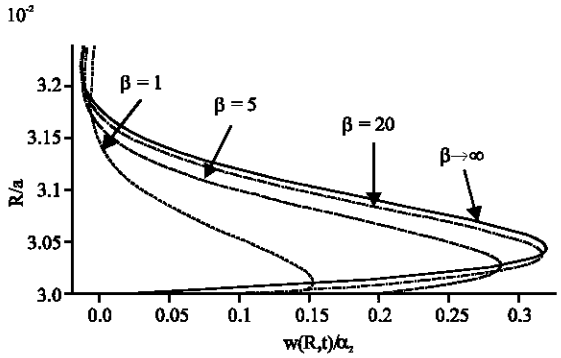

Fig. 14: w (R, t)/α_2 for t = $\pi/2\Omega_2$

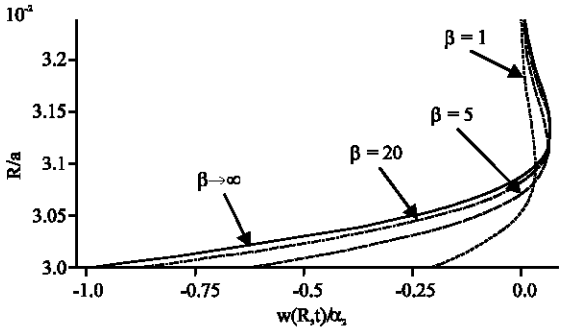

Fig. 15: w (R, t)/α_2 for t = π/Ω_2

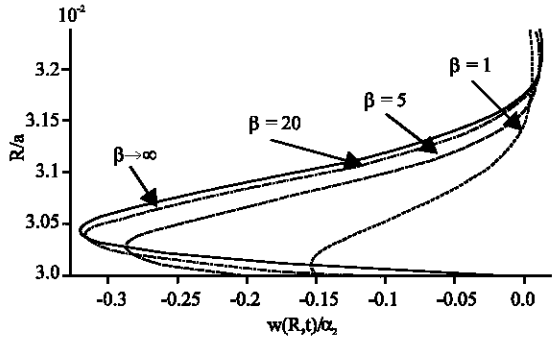

Fig. 16: w (R, t)/α_2 for t = $3\pi/2\Omega_2$

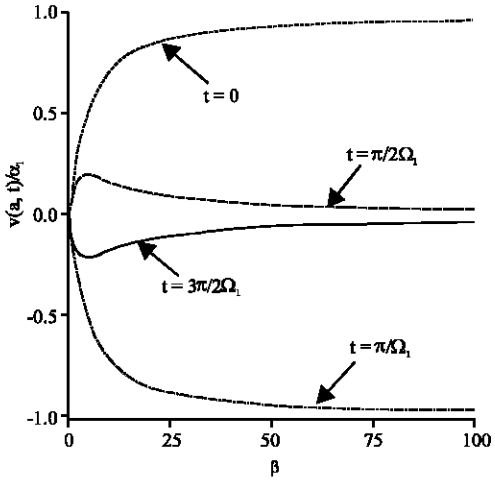

Fig. 17: v (a, t)/α_1 against β

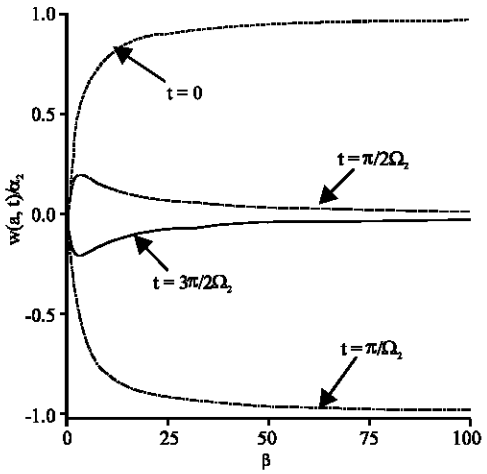

Fig. 18: w (a, t)/α_2 against β

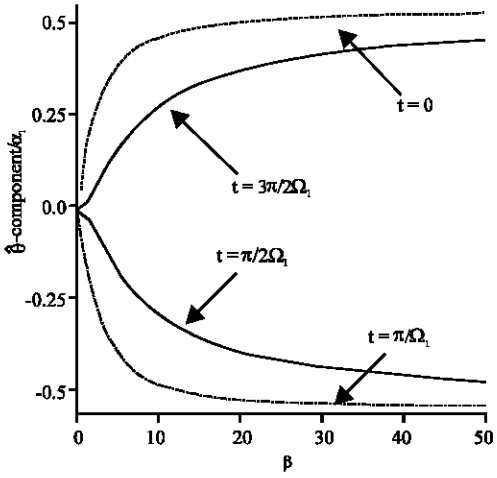

Fig. 19: $\hat{\theta}$-component/α_1 of the drag against β

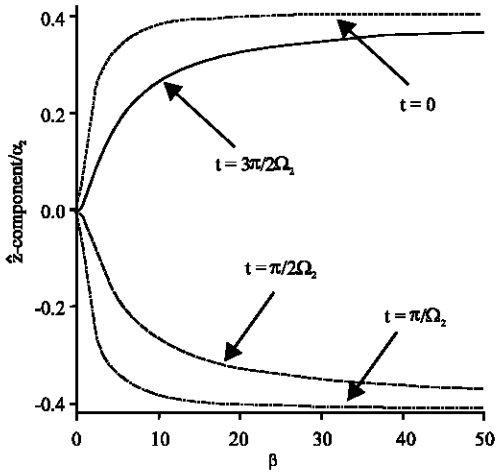

Fig. 20: $\hat{z}$-component/α_2 of the drag against β

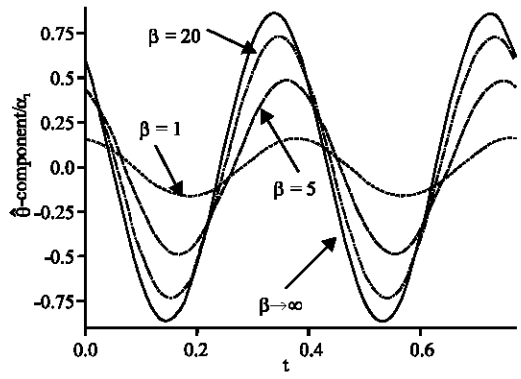

Fig. 21: $\hat{\theta}$-component/α_1 of the drag against t

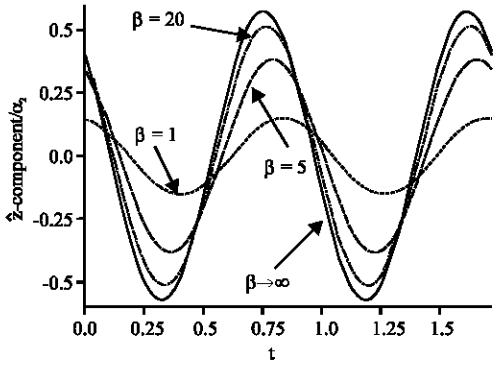

Fig. 22: $\hat{z}$-component/α_2 of the drag against t

It is of interest to compare the drag in each direction of oscillatory motion to determine which direction experiences greater drag. Thus, it can be shown that the difference in the magnitude of the components for the drag, given by Eq. 35, may be written as:

$$D_1 = 2\pi a\mu\beta\alpha_2\left[\left|\Re\left\{\left(\frac{\alpha_1}{\alpha_2}\right)\frac{\gamma_1\left(K_0(\gamma_1 a)+\frac{2K_1(\gamma_1 a)}{\gamma_1 a}\right)}{\mu\gamma_1 K_0(\gamma_1 a)+\left(\beta+\frac{2\mu}{a}\right)K_1(\gamma_1 a)}e^{i\Omega_1 t}\right\}\right| - \left|\Re\left\{\frac{\gamma_2 K_1(\gamma_2 a)}{\beta K_0(\gamma_2 a)+\mu\gamma_2 K_1(\gamma_2 a)}e^{i\Omega_2 t}\right\}\right|\right] \quad (48)$$

and further

$$\frac{D_1}{\alpha_2} = \left(\frac{\alpha_1}{\alpha_2}\right)\frac{D_1}{\alpha_1} \quad (49)$$

Based on Eq. 48 and 49, it suffices to only examine D_1/α_1 or D_1/α_2.

Figure 23-25 shows D_1/α_2 against β for $t = n\pi/2\Omega_1\Omega_2$, $n = 0,1,2,3$ for different values of α_1/α_2. It is observed that when $\alpha_1/\alpha_2 = 1/2$, the drag in the longitudinal direction of motion is greater than the drag in the torsional direction of motion for each value of t. Conversely, when $\alpha_1/\alpha_2 = 2$, the drag in the torsional direction of motion is greater than the drag in the longitudinal direction for the same values of t. It is also observed that when $\alpha_1/\alpha_2 = 1$, the drag in the torsional direction of motion is greater than the drag in the longitudinal direction of motion for $t = n\pi/2\Omega_1\Omega_2$, $n = 0,1,2$ but the opposite is observed when $t = 3\pi/2\Omega_1\Omega_2$.

It is noted that the drag in each direction is the same when:

$$D_1 = 0 \Rightarrow \frac{\alpha_1}{\alpha_2} = \frac{\left|\Re\left\{\frac{\gamma_2 K_1(\gamma_2 a)}{\beta K_0(\gamma_2 a)+\mu\gamma_2 K_1(\gamma_2 a)}e^{i\Omega_2 t}\right\}\right|}{\left|\Re\left\{\frac{\gamma_1\left(K_0(\gamma_1 a)+\frac{2K_1(\gamma_1 a)}{\gamma_1 a}\right)}{\mu\gamma_1 K_0(\gamma_1 a)+\left(\beta+\frac{2\mu}{a}\right)K_1(\gamma_1 a)}e^{i\Omega_1 t}\right\}\right|}$$

Figure 26-28 show D_1/α_2 against t for four different values of the slip parameter β for different values of α_1/α_2. It is observed that D_1/α_2 varies between positive and negative values, implying that the more efficient direction of motion keeps changing with the progression of time. Since,

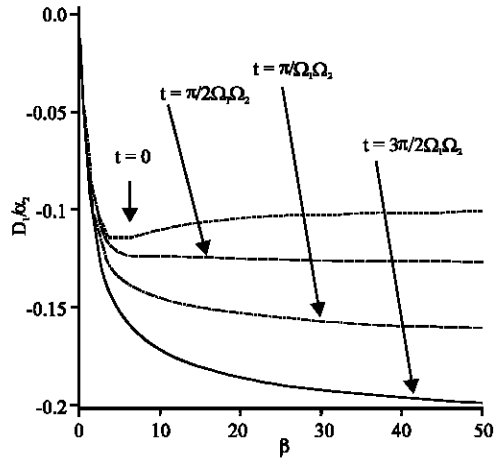

Fig. 23: D_1/α_2 against β for $\alpha_1/\alpha_2 = 1/2$

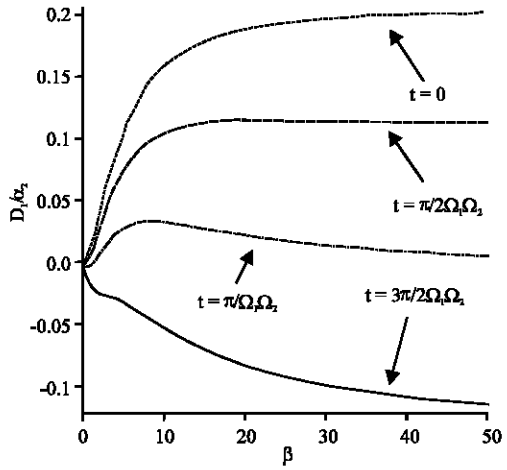

Fig. 24: D_1/α_2 against β for $\alpha_1/\alpha_2 = 1$

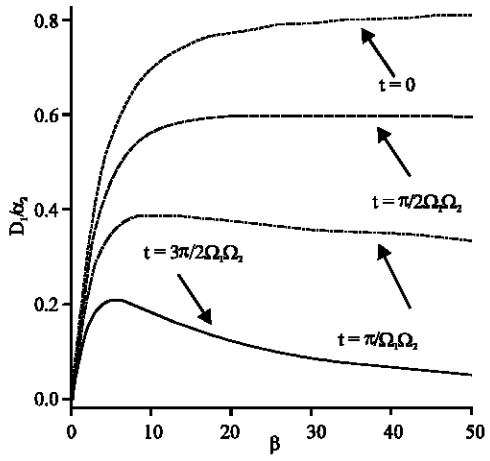

Fig. 25: D_1/α_2 against β for $\alpha_1/\alpha_2 = 2$

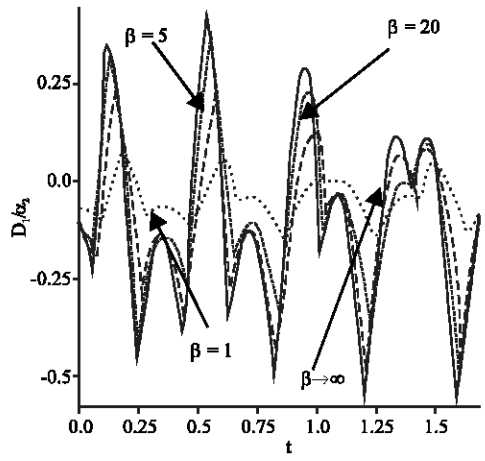

Fig. 26: D_1/α_2 against t for $\alpha_1/\alpha_2 = 1/2$

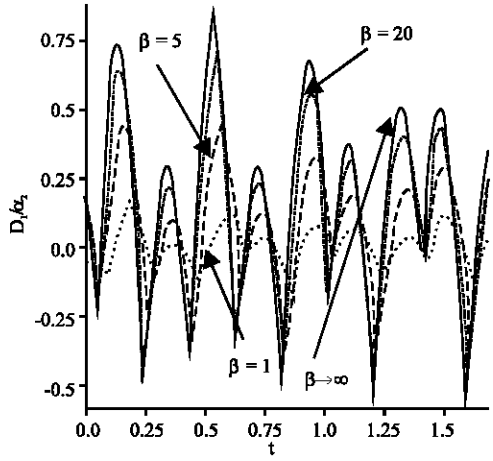

Fig. 27: D_1/α_2 against t for $\alpha_1/\alpha_2 = 1$

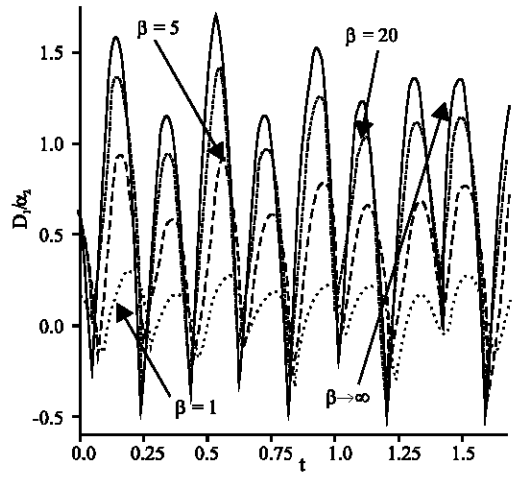

Fig. 28: D_1/α_2 against t for $\alpha_1/\alpha_2 = 2$

$$\frac{W_j}{\alpha_2^{\,2}} = \left(\frac{\alpha_1}{\alpha_2}\right)^2 \frac{W_j}{\alpha_1^{\,2}} \qquad (50)$$

then one needs to only examine

$$\frac{W_j}{\alpha_1^{\,2}} \text{ or } \frac{W_j}{\alpha_2^{\,2}}$$

to explore the behaviour of the work done by the drag force.

As β varies, the behaviour of the work done in each direction is shown in Fig. 29 and 30 for different values of α_1/α_2. It is observed in all cases that there is an increase in magnitude as β increases and using Eq. 37, it can be easily shown, as the graphs suggest that all tend to the limit:

$$\lim_{\beta\to\infty} \frac{W_j}{\alpha_2^{\,2}} = -\pi a \mu \Re \left[\frac{\gamma_1 \left(\frac{\alpha_1}{\alpha_2}\right)^2 \left(K_0(\gamma_1 a) + \frac{2K_1(\gamma_1 a)}{\gamma_1 a} \right)}{K_1(\gamma_1 a)} \hat{I}(\Omega_j, \Omega_1) + \frac{\gamma_2 K_1(\gamma_2 a)}{K_0(\gamma_2 a)} \hat{I}(\Omega_j, \Omega_2) \right]$$

CONCLUSION

Comparison of the work done in each direction of motion is now examined. Noting (50), it suffices to only examine

$$\frac{W_j}{\alpha_1^{\,2}} \text{ or } \frac{W_j}{\alpha_2^{\,2}}$$

From Fig. 31-33, it is observed in all cases that the magnitude of the work done in longitudinal direction is greater than the work done in the torsional direction.

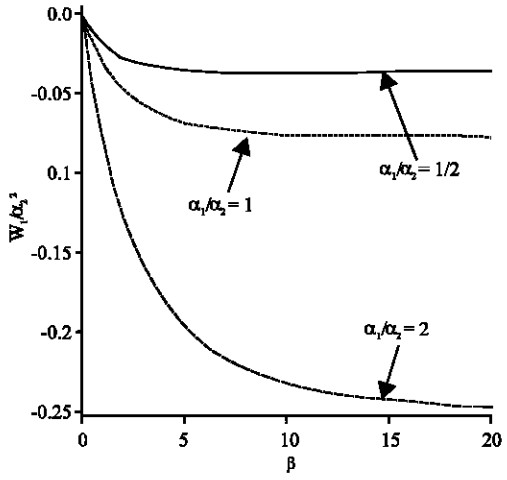

Fig. 29: $W_1/\alpha_2^{\,2}$ against β

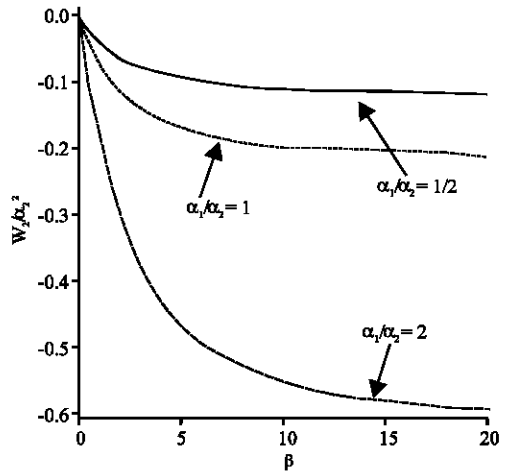

Fig. 30: $W_2/\alpha_2^{\,2}$ against β

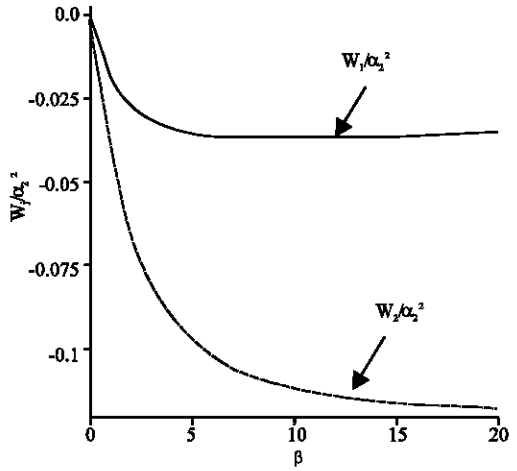

Fig. 31: $W_j/\alpha_2^{\,2}$ against β for $\alpha_1/\alpha_2 = 1/2$

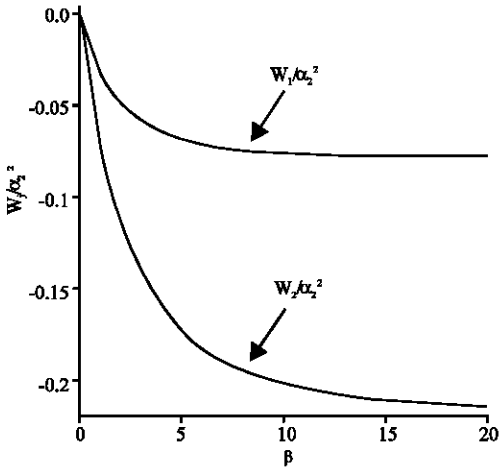

Fig. 32: $W_j/\alpha_2^{\,2}$ against β for $\alpha_1/\alpha_2 = 1$

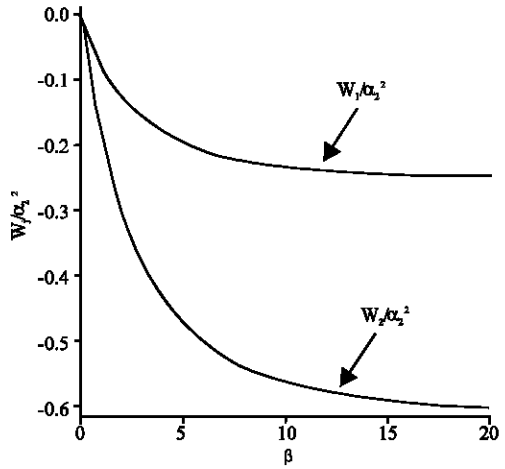

Fig. 33: W_j/α_2^2 against β for $\alpha_1/\alpha_2 = 2$

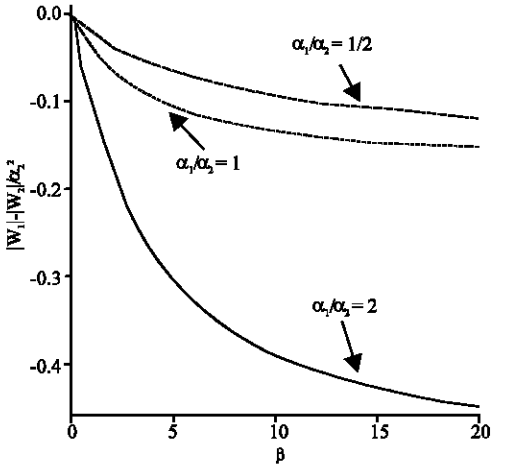

Fig. 34: $|W_1|-|W_2|/\alpha_2^2$ against β for $\alpha_1/\alpha_2 = 1/2, 1, 2$

Again noting (50), the behaviour of the difference in the work done in each direction, as β varies is displayed in Fig. 34. It is observed that the work done in the longitudinal direction is greater than the work done in the torsional direction, which is consistent with Fig. 31-33.

REFERENCES

Aleksandrov, O.E., S.P. Obraz, B.T. Porodnov, V.D. Seleznev and A.G. Flyagin, 1988. Thermal Polarization of a viscous gas flow accompanied by slip in a channel with a nonuniform surface. J. Eng. Phys. Thermophys., 55: 1098-1102.

Basset, A.B., 1961. A Treatise on Hydrodynamics. vol. 2, Dover Publ., New York.

Batchelor, G.K., 1967. An Introduction to Fluid Dynamics. Cambridge University Press, Cambridge, ISBN-10: 0521663962.

Casarella, M.J. and P.A. Laura, 1969. Drag on an oscillating rod with longitudinal and torsional motion. J. Hydronautics, 3: 180-183.

Gad-el-Hak, M., 1999. The fluid mechanics of microdevices-the freeman scholar lecture. J. Fluids Eng., 121: 5-33.

LMNO Engineering, Research and Software, Ltd., 1999. Fluid properties-density and kinematic viscosity of liquids and gases: Water, seawater, oil, gasoline, mercury, air, carbon dioxide, nitrogen, helium. Table of Fluid Properties (Liquids and Gases). http://www.lmnoeng.com/fluids.htm.

Morinishi, K., 2006. Numerical simulation for gas microflows using Boltzmann equation. Comput. Fluids, 35: 978-985.

Owen, D. and K. Rahaman, 2006. On the flow of an Oldroyd-B liquid through a straight circular tube performing longitudinal and torsional oscillations of different frequencies Math: Ensenanza Univ., 14: 35-43.

Rahaman, K., 2004. Internal flow due to the longitudinal and torsional oscillation of a cylinder. Asia J. Inform. Technol., 3: 985-991.

Rahaman, K., 2005. Non-newtonian flow due to a solid oscillating rod. Asia J. Inform. Technol., 4: 243-249.

Rajagopal, K.R., 1983. Longitudinal and torsional oscillations of a rod in a non-newtonian fluid. Acta Mech., 49: 281-285.

Ramkissoon, H. and S.R. Majumdar, 1990. Flow due to the longitudinal and torsional oscillation of a cylinder. J. Applied Math. Phys., 41: 598-603.

Ramkissoon, H., C.V. Easwaran and S.R. Majumdar, 1991. Longitudinal and torsional oscillation of a rod in a polar fluid. Int. J. Eng. Sci., 29: 215-221.

Schaaf, S.A. and P.L. Chambre, 1961. Flow of Rarefied Gases. Princeton University Press, Princeton NJ, USA., ISBN-10: 0691079641.